

# Constitutive Matrices Using Hexahedra in a Discrete Approach for Eddy Currents

Patrick Dular<sup>1</sup>, Ruben Specogna<sup>2</sup>, and Francesco Trevisan<sup>2</sup>

<sup>1</sup>Belgian National Fund for Scientific Research (F.N.R.S.) and the Department of Electrical Engineering and Computer Science, Unit of Applied Electricity, University of Liege, Montefiore Institute—B28, B-4000 Liege, Belgium

<sup>2</sup>Dipartimento di Ingegneria Elettrica, Gestionale e Meccanica, Università di Udine, I-33100 Udine, Italy

We examine the construction of reluctivity and Ohm's constitutive matrices for discrete geometric approaches using nonregular hexahedra as primal volumes. The effect of element deformation on the representation of uniform fields have been investigated for static fields. Then convergence and accuracy of the proposed matrices has been carried out using an eddy-current problem as working example.

**Index Terms**—Constitutive matrices, discrete geometric approaches, eddy-currents.

## I. INTRODUCTION

DISCRETE geometric approaches [1] like the Finite Integration Technique (FIT) [2] or the Cell Method [3], [4] have been originally implemented using regular hexahedra to construct the primal cell complex. In recent years the FIT approach has been extended to distorted hexahedra [5]. In the case of the Cell Method, the difficulty for nonregular hexahedra lies in the construction of constitutive matrices, the discrete counterparts of constitutive laws.

The aim of this paper is to construct constitutive matrices—the reluctance  $\nu$  mapping magnetic fluxes to m.m.f.s and conductance matrix  $\sigma$  mapping e.m.f.s to currents—for nonregular hexahedra. This shifts the emphasis on the basis functions to employ. Even though no canonical edge and face elements do exist for hexahedra, we used the basis functions described in [6]. Then we will follow the recipe to construct constitutive matrices proposed in [7] for simplexes.

As a first step, the effect on the solution of the distortion of the element will be investigated with respect to uniform static current conduction and magnetic fields using an extremely coarse mesh. Then an eddy current problem will serve as a working example for the case of nonuniform fields and deformed hexahedra. The numerical results will be compared with a tetrahedral mesh using the discrete geometric approach.

## II. CELL COMPLEXES AND BASIS FUNCTIONS

The inner-oriented geometric elements<sup>1</sup> of the primal complex  $\mathcal{K}$  are the nodes  $n$ , edges  $e$ , faces  $f$  and volumes  $v$  of a hexahedra-based mesh (Fig. 1).

We will focus here on the the nodal, edge, and face mixed finite elements [6], associated with the geometric elements of  $\mathcal{K}$ . We indicate with  $s_{n_i}(p)$  the nodal function<sup>2</sup> of the point  $p \in v$

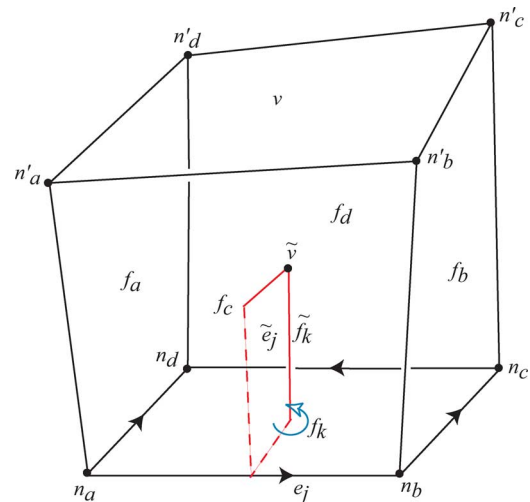


Fig. 1. Nonregular hexahedron is shown, together with the oriented geometric elements forming the primal  $\mathcal{K}$  and the dual  $\tilde{\mathcal{K}}$  cell complexes.

of coordinates  $(x, y, z)$ , associated with the node  $n_i$ . It is equal to 1 when  $p = n_i$  and it is null on the other nodes.

Edge vector function  $s_{e_j}(p)$  attached to edge  $e_j$ , inner oriented from nodes  $n_a$  to  $n_b$  (refer to Fig. 1), is defined as

$$s_{e_j} = s_{n_b} \nabla F_b - s_{n_a} \nabla F_a \quad (1)$$

where  $F_a = s_{n_a} + s_{n_d} + s_{n'_a} + s_{n'_d}$  is the sum of the nodal functions  $s_{n_i}$  associated with the four nodes  $(n_a, n_d, n'_a, n'_d)$  individuating the face  $f_a$ , this face has node  $n_a$  as the only common node with edge  $e_j$ . Similarly we have that  $F_b = s_{n_b} + s_{n_c} + s_{n'_b} + s_{n'_c}$  holds, where the nodal functions  $s_{n_i}$  are associated with the four nodes of face  $f_b$ , having node  $n_b$  in common with edge  $e_j$ .

Finally, face vector function  $s_{f_k}(p)$  associated with face  $f_k$ , inner oriented as shown in Fig. 1, is defined as

$$s_{f_k} = s_{n_a} \nabla F_a \times \nabla F_c + s_{n_b} \nabla F_c \times \nabla F_b + s_{n_c} \nabla F_b \times \nabla F_d + s_{n_d} \nabla F_d \times \nabla F_a \quad (2)$$

where  $\nabla F_a \times \nabla F_c$  involves  $F_a$  associated with the four nodes of face  $f_a$  and  $F_c = s_{n_a} + s_{n_b} + s_{n'_a} + s_{n'_b}$  associated with the four nodes of face  $f_c$  respectively (refer to Fig. 1); the pair of faces  $f_a, f_c$  has the node  $n_a$  in face  $f_k$  in common. The pair

Digital Object Identifier 10.1109/TMAG.2007.916230

Color versions of one or more of the figures in this paper are available online at <http://ieeexplore.ieee.org>.

<sup>1</sup>The notion of inner and outer orientations can be found in [3] and [9].

<sup>2</sup>In our case  $s_{n_i}(p)$  is generated by the following polynomial base  $(1, x, y, z, xy, xz, yz, xyz)$ .

of gradient vectors  $\nabla F_a, \nabla F_c$ , appearing in the cross product, is ordered according to the order of the faces  $f_a, f_c$  they are associated with; the order of these faces is established by the inner orientation of face  $f_k$  and then, in our case,  $f_a$  comes as first. Similarly for the other cross products.

These scalar and vector functions form a basis for the spaces they generate and they reduce to the Whitney edge and face vector functions when  $v$  degenerates to a tetrahedron.

It is a standard procedure to introduce a reference cube  $v'$  and an injective map  $T, T(p') \mapsto p$  mapping a point  $p' \in v'$  of coordinates  $\xi, \eta, \zeta$  in the reference cube  $v'$  into the point  $p$  in the actual hexahedron  $v$ . We use this mapping to systematically compute the edge and face vector functions exploiting the Jacobian matrix of  $T$ .

The dual complex  $\tilde{\mathcal{K}}$  consists of outer-oriented geometric elements. A generic geometric element  $\alpha$  will be obtained by mapping the points forming the corresponding geometric element  $\alpha'$  of  $v'$  as  $\alpha = T(\alpha')$ . We refer to a primal cell complex made of a single hexahedron  $v$ . A dual node  $\tilde{v}$  is obtained by mapping the barycenter  $g_{v'}$  of the reference cube  $v'$  into the point  $\tilde{v} = T(g_{v'})$  in  $v$ . Note that, in general,  $\tilde{v}$  is no more the barycenter of  $v$ . A dual edge  $\tilde{f}$  is a segment in  $v$  such that  $\tilde{f} = T(\tilde{f}')$ , where  $\tilde{f}'$  is a segment in  $v'$  joining  $g_{v'}$  and the barycenter  $g_{f'}$  of face (a square)  $f'$  corresponding to  $f$  in  $v$ . Again note that  $\tilde{f}$  is a segment between points  $\tilde{v}$  and  $T(g_{f'})$ , but  $T(g_{f'})$  is not the barycenter of face  $f$ . For this reasons the resulting dual complex is not the barycentric one in general, but it is barycentric only in the reference cube  $v'$ . A dual face  $\tilde{e}$  is a nonplane quadrilateral surface defined as  $\tilde{e} = T(\tilde{e}')$ , where  $\tilde{e}'$  is the corresponding dual face (a square) in  $v'$ . Finally a dual volume  $\tilde{n}$  is bounded by the dual faces around  $n$ .

### III. CONSTITUTIVE MATRICES

Constitutive matrices are discrete counterparts of the Hodge operator, [8], [9]. We will focus here on reluctance  $\boldsymbol{\nu}$  and on conductance  $\boldsymbol{\sigma}$  constitutive matrices. The matrix  $\boldsymbol{\nu}$  maps an array of fluxes  $\Phi$  over the primal faces to an array  $\mathbf{F}$  of m.m.f.s on the dual edges. Its dimension equals the number  $\mathcal{F}$  of primal faces. The matrix  $\boldsymbol{\sigma}$  maps an array  $\mathbf{U}$  of e.m.f.s along primal edges to an array of currents crossing the dual faces and its dimension is the number of primal edges  $\mathcal{E}$  of the conducting region.

In order to construct these matrices, we will extend to hexahedra the technique described in [7] for the case of simplexes. In the following we will consider the cell complexes  $\mathcal{K}, \tilde{\mathcal{K}}$  formed by a single hexahedron. We also assume reluctivity  $\nu$  and conductivity  $\sigma$  element-wise uniform. The matrices  $\boldsymbol{\nu}$  and  $\boldsymbol{\sigma}$  for a mesh of hexahedra are obtained by summing up the contribution element by element.

#### A. Reluctance Matrix

We indicate with  $\Phi_k$  the flux attached to a primal face  $f_k$  of hexahedron  $v$ , with  $k = 1, \dots, 6$ . Using face vector functions  $s_{f_k}$ , we may approximate the flux density vector in  $v$  as

$$\mathbf{B}^s = \sum_{k=1}^6 s_k^f \Phi_k. \quad (3)$$

Then, from constitutive law between fields  $\mathbf{H} = \nu \mathbf{B}$ , the m.m.f.  $F_h$  along dual edge  $\tilde{f}_h$  in  $v$ , with  $h = 1, \dots, 6$ , becomes  $F_h = \sum_{k=1}^6 \Phi_k \int_{\tilde{f}_h} \nu s_k^f \cdot d\mathbf{l}$ . Finally, the numbers

$$\nu_{hk} = \int_{\tilde{f}_h} \nu s_k^f \cdot d\mathbf{l} \quad (4)$$

are the entries of a possible  $6 \times 6$   $\boldsymbol{\nu}$  matrix.

#### B. Conductance Matrix

In a similar way, but at a different geometric level, we indicate with  $U_j$  the e.m.f. along a primal edge  $e_j$  of hexahedron  $v$ , with  $j = 1, \dots, 12$ . Then from edge vector functions  $s_{e_j}$ , we may approximate the electric field vector in  $v$  as

$$\mathbf{E}^s = \sum_{j=1}^{12} s_j^e U_j. \quad (5)$$

Combining it with Ohm's law between fields  $\mathbf{J} = \sigma \mathbf{E}$ , the current density in  $v$  becomes  $\mathbf{J} = \sum_{j=1}^{12} U_j \int_{\tilde{e}_i} \sigma s_j^e \cdot d\mathbf{s}$ . Then the numbers

$$\sigma_{ij} = \int_{\tilde{f}_i} \sigma s_j^e \cdot d\mathbf{a} \quad (6)$$

are the entries of a possible  $12 \times 12$   $\boldsymbol{\sigma}$  matrix.

### IV. EFFECT OF THE ELEMENT DEFORMATION

We will face here a numerical analysis of the effect on the solution of the deformation of an hexahedron without modifying significantly its size. To this aim, we consider the static case, where the actual fields are uniform; later we will move to quasi-static.

To quantify the extent of this effect, we will evaluate the quantity associated with field  $\mathbf{X}$

$$\epsilon_X = \frac{\int_D m |\mathbf{X}^s - \mathbf{X}|^2 dv}{\int_D m |\mathbf{X}|^2 dv} \quad (7)$$

where  $\mathbf{X}^s$  indicates the approximated vector field,  $\mathbf{X}$  is the actual field,  $D$  is the problem domain and  $|\bullet|$  is the amplitude of a vector field. The vector field  $\mathbf{X}$  stands for  $\mathbf{B}$  or  $\mathbf{E}$  and the approximated field  $\mathbf{X}^s$  is given by (3) or (5) correspondingly; reluctivity or conductivity are represented by  $m$  according to the case.

As working examples, we consider a magnetostatic (MA) and a current conduction (CC) problems in the domain  $D$ , formulated in a discrete way as [10]

$$\mathbf{C}^T \boldsymbol{\nu} \mathbf{C} \mathbf{A} = \mathbf{0} \quad (\text{MA}), \quad \mathbf{G}^T \boldsymbol{\sigma} \mathbf{G} \mathbf{V} = \mathbf{0} \quad (\text{CC}) \quad (8)$$

where  $\mathbf{C}, \mathbf{G}$  are incidence matrices between the pairs  $(f, e)$  and  $(e, n)$  of the primal complex,  $\mathbf{A}$  is the array of the circulations of the magnetic vector potential associated with the primal edges and  $\mathbf{V}$  is the array of the electric scalar potentials associated with the primal nodes. The sources are assigned by specifying proper boundary conditions, for this reason the right-hand sides in (8) are null. Finally,  $\dim(\boldsymbol{\nu}) = \mathcal{F}$  and  $\dim(\boldsymbol{\sigma}) = \mathcal{E}$ .

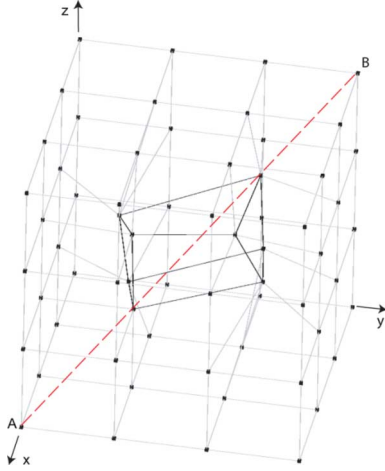


Fig. 2. Primal complex  $\mathcal{K}'$  consisting of distorted hexahedra. The considered distortion produces 26 hexahedra; the element having node A as one of its nodes remains a cube.

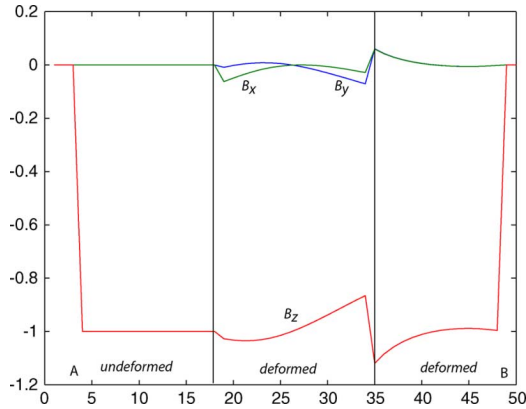


Fig. 3. Three components  $B_x$ ,  $B_y$ ,  $B_z$ , are shown computed along the line AB; note that no error occurs in the undistorted element.

The boundary conditions have been set in order to generate in  $D$  a uniform magnetic induction field of amplitude  $B = 1$  T and a uniform current density field of amplitude  $J = 4 \cdot 10^7$  A/m<sup>2</sup> respectively, both directed as the  $z$  axis. In the domain  $D$ —a cube of unitary edge—we constructed an undistorted primal complex  $\mathcal{K}$  consisting of  $3 \times 3 \times 3$  cubical elements. By displacing five nodes but one of the innermost cube, we obtain a new deformed primal complex  $\mathcal{K}'$  made of 26 hexahedra plus one cube (see Fig. 2).

A first result is that the stiffness matrices in (8) are symmetric and positive definite, for the undistorted primal complex  $\mathcal{K}$  and we have that the errors  $\epsilon_B$ ,  $\epsilon_E$  are both null. However, the same matrices become nonsymmetric for the distorted primal complex  $\mathcal{K}'$  and we have that  $\text{asy}(\mathbf{G}^T \boldsymbol{\sigma} \mathbf{G}) = 7.5\%$ ,  $\text{asy}(\mathbf{C}^T \boldsymbol{\nu} \mathbf{C}) = 9.7\%$  hold respectively, where  $\text{asy}(\mathbf{X}) = \|\mathbf{X} - \mathbf{X}^T\| / \|\mathbf{X}\|$  indicates the extent of the nonsymmetry of matrix  $\mathbf{X}$  and  $\|\bullet\|$  is the  $\infty$ -norm. Correspondingly the error  $\epsilon_E$  is null indicating that  $\boldsymbol{\sigma}$  exactly represents a uniform field. In the case of a MA problem the error becomes  $\epsilon_B = 15\%$ . This indicates that face vector functions  $s_k^f$  are unable to represent a uniform vector field when a deformation of the elements occurs. To see this effect—known in the framework of finite elements too—we plotted in Fig. 3 the three components of the magnetic induction  $\mathbf{B}$  in a number

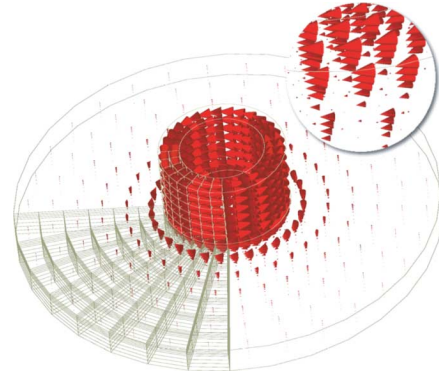


Fig. 4. Real parts of the current densities vectors in the stranded coil placed above a conducting aluminium plate are shown for a mesh of 15 540 hexahedra. The amplitude of the current density vector in the coil is scaled. A zoom to see the skin effect is also shown.

of points evenly distributed along the line AB drawn in Fig. 2. However, it is interesting to note that a uniform  $\mathbf{B}$  field in the MA problem is exactly represented when it is computed in the special point  $\tilde{v}$  even in the presence of a large deformation of the hexahedron.

We also computed the ratio between the maximum and the minimum eigenvalues of the stiffness matrices appearing in (8), before the boundary conditions are imposed. We denote with  $c(\mathbf{X})$  this ratio associated with matrix  $\mathbf{X}$ .

Then we have that  $c(\mathbf{C}^T \boldsymbol{\nu} \mathbf{C}) = 8.59$  and  $c(\mathbf{G}^T \boldsymbol{\sigma} \mathbf{G}) = 13.04$  respectively; on the other hand  $c'(\mathbf{C}^T \boldsymbol{\nu} \mathbf{C}) = 13.91$  and  $c'(\mathbf{G}^T \boldsymbol{\sigma} \mathbf{G}) = 19.64$  hold for the case of  $\mathcal{K}'$ . This shows that the deformation of the elements affects in a comparable way the ill-conditioning of the final systems in (8).

## V. CONVERGENCE FOR MAGNETO-QUASI-STATICS

We consider here an eddy current problem as working example to study the convergence and accuracy of the constitutive matrices  $\boldsymbol{\nu}$ ,  $\boldsymbol{\sigma}$  when fields are no more element wise uniform and the elements forming the primal complex are distorted.

The domain of interest  $D$  of the eddy-current problem (a cylinder of diameter of 60 mm and height 44.5 mm), has been partitioned into a source region  $D_s$  (a circular current driven coil of 18 mm of outer diameter, 12 mm of inner diameter, and 10 mm height) placed above a conducting region  $D_c$  consisting of an aluminium plate 4 mm thick and with a radius of 30 mm (Fig. 4). The insulating region  $D_a$  is the complement of  $D_c$  and  $D_s$  in  $D$ . In  $D_s$  we force a sinusoidal current source  $I_s = \sin(\omega t)$  with a frequency of  $f = 5$  kHz.

We briefly recall the basic equations of a discrete geometric approach to solve eddy-current problems<sup>3</sup> [11] [12], [13]. We search for the array  $\mathbf{A}$  of the circulations of the magnetic vector potential along primal edges  $e$  of  $D$  and for the array  $\boldsymbol{\chi}$  of scalar potential  $\chi$  associated with primal nodes  $n$  of  $D_c$  such that

$$\begin{aligned} (\mathbf{C}^T \boldsymbol{\nu} \mathbf{C} \mathbf{A})_e &= (\mathbf{I})_e \quad \forall e \in D \\ (\mathbf{C}^T \boldsymbol{\nu} \mathbf{C} \mathbf{A})_e + i\omega(\boldsymbol{\sigma} \mathbf{A}_c)_e + i\omega(\boldsymbol{\sigma} \mathbf{G} \boldsymbol{\chi})_e &= 0 \quad \forall e \in D_c \\ i\omega(\mathbf{G}^T \boldsymbol{\sigma} \mathbf{A})_n + i\omega(\mathbf{G}^T \boldsymbol{\sigma} \mathbf{G} \boldsymbol{\chi})_n &= 0 \quad \forall n \in D_c \end{aligned} \quad (9)$$

<sup>3</sup>The proposed formulation is part of the Geometric Approach for Maxwell's Equations (GAME) code developed by R. Specogna and F. Trevisan with the partial support of MIUR (Italian Ministry for University and Research).

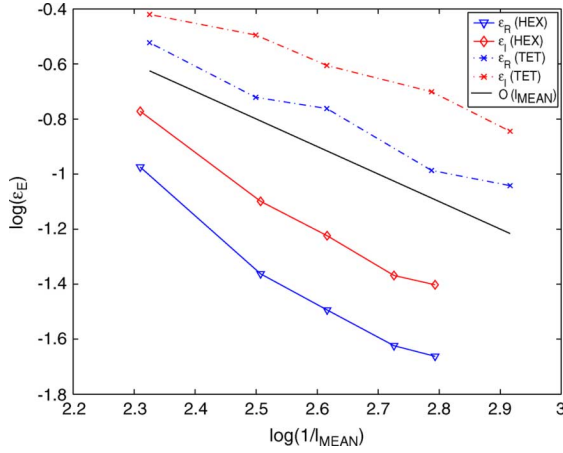


Fig. 5. Convergence in terms of  $\epsilon_E$  is compared for the case of hexahedra and tetrahedra; the  $O(l_{MEAN})$  reference convergence order is drawn in addition as a continuous line.

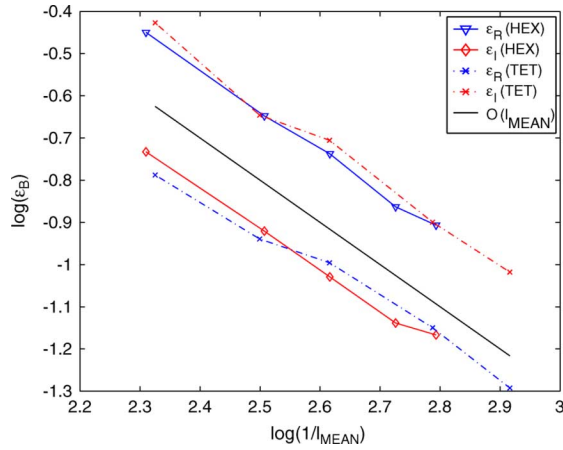


Fig. 6. Convergence in terms of  $\epsilon_B$  is compared for the case of hexahedra and tetrahedra; the  $O(l_{MEAN})$  reference convergence order is drawn in addition as a continuous line.

where array  $\mathbf{A}_c$  is the subarray of  $\mathbf{A}$ , associated with primal edges in  $D_c$ ; the matrix  $\mathbf{G}$  is associated with pairs  $(e, n)$  of  $D_c$ . With  $(\mathbf{x})_k$  we mean the  $k$ th row of array  $\mathbf{x}$ , where  $k = \{e, n\}$  is the label of edge  $e$  or of node  $n$ . Finally  $\dim(\boldsymbol{\nu}) = \mathcal{F}$  and  $\dim(\boldsymbol{\sigma}) = \mathcal{E}_c$ ,  $\mathcal{E}_c$  being the number of edges in  $D_c$ . The system (9) is singular and to solve it we rely on CG method without gauge condition [14].

The test problem has axial symmetry and the results obtained from the 3-D analysis in terms of the errors  $\epsilon_B$  and  $\epsilon_E$ , have been compared with respect to a 2-D model. To study the convergence, we used five meshes with increasing refinement, having 1536, 6156, 11 776, 25 800, and 39 168 hexahedral cells respectively. We choose the mean length ( $l_{MEAN}$ ) of the edges as

quality factor for the mesh. Figs. 5 and 6 show that the convergence is of the first order. Moreover the convergence has been computed not only for hexahedra but also for the case of a primal complex made of tetrahedra, where the constitutive matrices can be computed as described in [12], [13]. To achieve a similar accuracy in the solution, a mesh of about 39 000 hexahedra is needed while, in the case of tetrahedra, 360 000 elements are required.

## VI. CONCLUSION

Even though we started from the same basis functions as in the framework of finite elements, to construct the reluctance and conductance constitutive matrices, the final stiffness matrices are different. They are in general nonsymmetric, the extent of the asymmetry depending on the deformation of the element. The investigation of the effect on the solution of the element deformation reveals that only the face vector functions—used to construct the  $\boldsymbol{\nu}$  matrix—are unable to represent a uniform field in points different from  $\hat{\nu}$ , where however the representation is exact. Finally an eddy current problem, used to investigate the convergence for nonuniform fields, revealed a first-order convergence, but requiring about a factor of 10 elements less with respect to a tetrahedra mesh to achieve the same accuracy.

## REFERENCES

- [1] Bossavit, *IEEE Trans. Magn.*, vol. 34, no. 5, pp. 2429–2432, 1998.
- [2] T. Weiland, *Int. J. Numer. Model.*, vol. 9, pp. 295–319, 1996.
- [3] E. Tonti, in *Int. Workshop Electr. Magn. Fields*, Marseille, France, May 12–15, 1998, pp. 284–294.
- [4] E. Tonti, *IEEE Trans. Magn.*, vol. 38, no. 2, pp. 333–336, 2002.
- [5] M. Clemens and T. Weiland, *PIER Monograph Series*, vol. 32, pp. 65–87, 2001.
- [6] P. Dular, J.-Y. Hody, A. Nicolet, A. Genon, and W. Legros, *IEEE Trans. Magn.*, vol. 30, no. 5, pp. 2980–2983, 1994.
- [7] T. Tarhasaari, L. Kettunen, and A. Bossavit, *IEEE Trans. Magn.*, vol. 35, no. 3, pp. 1494–1497, 1999.
- [8] A. Bossavit and L. Kettunen, *IEEE Trans. Magn.*, vol. 36, no. 4, pp. 861–867, 2000.
- [9] A. Bossavit, *Computational Electromagnetism*. New York: Academic, 1998.
- [10] F. Trevisan and L. Kettunen, *IEEE Trans. Magn.*, vol. 40, pp. 361–365, 2004.
- [11] F. Trevisan, *IEEE Trans. Magn.*, vol. 40, no. 2, pp. 1314–1317, 2004.
- [12] F. Trevisan and L. Kettunen, “Geometric interpretation of finite dimensional eddy current formulations,” *Int. J. Numer. Meth. Eng.*, vol. 67, no. 13, pp. 1888–1908, 2006.
- [13] R. Specogna and F. Trevisan, *IEEE Trans. Magn.*, vol. 41, no. 4, pp. 1259–1263, 2005.
- [14] A. Kameari and K. Koganezawa, *IEEE Trans. Magn.*, vol. 33, no. 2, pp. 1223–1226, 1997.